Polymer gel dosimetry of an electron beam in the presence of a magnetic field

Polymer gel dosimetry of an electron beam in the presence of a magnetic field

J Vandecasteele[1] and Y De Deene[1,2]
[1]Department for Radiation Oncology and Experimental Cancer Research, Ghent University, De Pintelaan 185, 9000 Gent, Belgium
[2]Institute of Medical Physics, School of Physics, University of Sydney, Sydney NSW, Australia

E-mail: Jan.Vandecasteele@UGent.be

Abstract. The effect of a strong external magnetic field on 4 MeV electron beam was measured with polymer gel dosimetry. The measured entrance dose distribution was compared with a calculated fluence map. The magnetic field was created by use of two permanent Neodymium (NdFeB) magnets that were positioned perpendicular to the electron beam. The magnetic field between the magnets was measured with Hall sensors. Based on the magnetic field measurement and the law of Biot-Savart, the magnetic field distribution was extrapolated. Electron trajectories were calculated using a relativistic Lorentz force operator. Although the simplified computational model that was applied, the shape and position of the calculated entrance fluence map are found to be in good agreement with the measured dose distribution in the first layer of the phantom. In combination with the development of low density polymer gel dosimeters, these preliminary results show the potential of 3D gel dosimetry in MRI-linac applications.

1. Introduction

In recent times, MRI scanners were combined with high energy x-ray treatment devices creating so called MRIGRT [1-3]. This combination results in the presence of a strong magnetic field in a region where charged particles are created, thus affecting the dose distribution inside a patient. A preliminary study was set-up to investigate the potential use of polymer gel dosimeters (both unit density and lung equivalent gel dosimeters [4]) in the presence of a strong magnetic field. A simulation program was developed to predict the charged particles trajectories in vacuum in the presence of an electromagnetic field.

2. Materials and methods

2.1. Gel fabrication

The PAGAT dosimeter used in this study, is composed of gelatin (6% w/w), acrylamide (3% w/w), N,N'-methylene-bis-acrylamide (3% w/w) and 5 mM Bis[tetrakis(hydroxymethyl)phosphonium] sulphate (THPS) as antioxidant. The polymer gel was fabricated according to a procedure as described elsewhere [5]. The gel was at 32 °C when it was poured in 21 test tubes and two Barex™ containers (20 x 20 x 6 cm^3).

2.2. Irradiation

Two PAGAT gel dosimeters were irradiated with a 4 MeV electron beam (4 x 1 cm² at isocentre) from a clinical linear accelerator (Elekta Synergy). The first phantom was irradiated in the presence of a magnetic field (figure 1b and 1c). A dedicated magnet holder was constructed to position the NdFeB magnets 3.3 cm from each other. In between the magnets sufficient space was left to allow the electron beam to pass (figure 1c). The second PAGAT gel dosimeter was irradiated at the same distance from the source, but without the presences of the magnets.

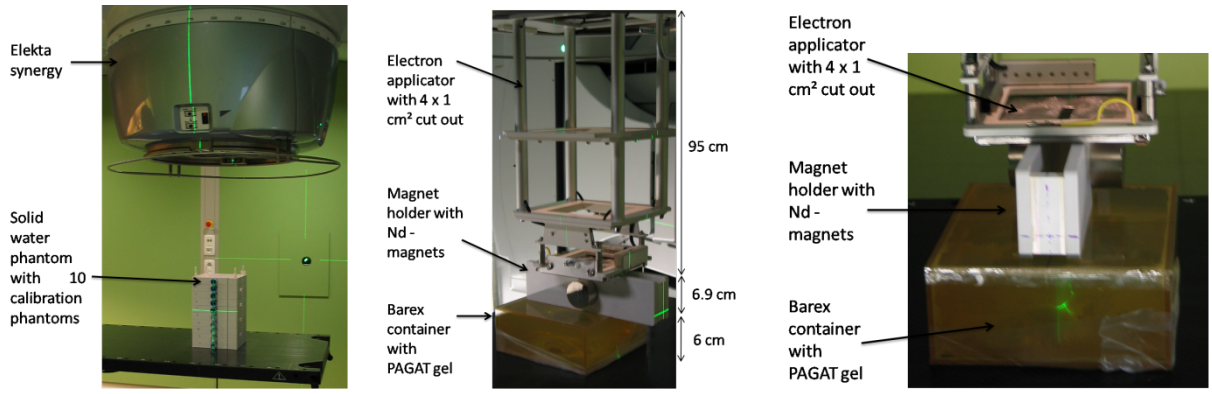

Figure 1: A set of calibration phantoms was irradiated with a 6 MV photon beam using a dedicated solid water phantom (a). Set-up of the irradiation of a gel phantom with an 4 MeV electron beam in the presence of 2 magnets (b). An appropriate cut-out was placed in the electron applicator assuring that the 4 x 1 cm² beam passes through the space between the 2 magnets (c).

A set of 8 calibration phantoms was irradiated in a solid water phantom with a 6 MV photon beam with field size 10 x 10 cm² and SSD 90 cm (figure 1a). In this phantom, 10 calibration phantoms can be positioned along the depth of the irradiation beam. An ion chamber measurement was performed at each position in the solid water phantom and compared to in-house beam data for the same irradiation setup in water. Finally, five calibration phantoms were irradiated with a 4 MeV electron beam under reference conditions so that 1 MU equals 1 cGy. This allowed us to compare the response of the gel to a photon beam exposure versus the response of the gel to an electron beam exposure.

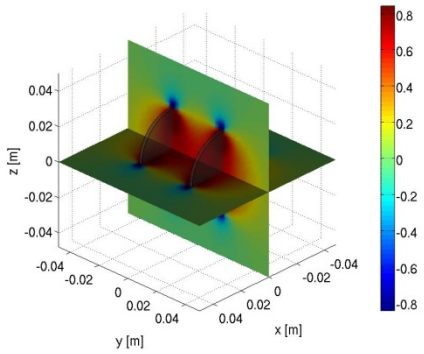

Figure 2: The calculated magnetic field distribution expressed in Tesla around the magnets. The magnets are represented in the figure by two round discs.

2.3. Computer simulations

The magnetic field generated by the two NdFeB magnets was calculated using the law of Biot-Savart (figure 2). The magnitude of the magnetic field was independently calibrated by Hall sensor probe measurements of the magnetic field generated by the two magnets. The magnetic field strength

amounts to 0.49 Tesla in between the two magnets. The electron beam trajectories were predicted by a relativistic calculation of the Lorentz force exerted on the charged particles in the presence of the electromagnetic field. Because no in-house data on the energy spectrum of the 4 MeV electron beam was available, literature values were used [6]. No particle interactions with matter were included in the our simulations.

2.4. MRI read-out

Quantitative NMR spin-spin relaxation rate (R_2) maps were recorded using a multiple spin-echo sequence with 32 spin-echoes with a 1.5 Tesla MRI scanner (Siemens Avanto). The phantoms were separately scanned in the body coil along with the calibration phantoms using following imaging parameters: TR: 3000 ms:, TE: 40 – 1280 ms, voxel size: 1 × 1 × 3 mm^3, number of acquisitions: 4 and bandwidth: 130 Hz/pixel. The centre of the recorded slice was positioned at 8 mm from the top of the phantom (including 4 mm Barex™). A fitting of the intensity of 31 equidistant consecutive base images to a monoexponential decay using χ^2-minimalisation was performed to obtain R_2 maps [7]. R_2 maps were calibrated to dose maps using the dose-R_2 relationship extracted from the calibration phantoms.

3. Results and discussion

3.1. Calibration

The dose-R_2 response of the calibration phantoms irradiated with a 6 MV photon beam (figure 3, blue markers) matches the dose-R_2 response of those irradiated with the 4 MeV electron beam (figure 3, red markers). The novel solid water phantom is an easy, reproducible and fast set-up to irradiate a set of calibration vials to a known dose. However, because the 10 calibration vials are positioned underneath each other, the effect of the accumulating borosilicate glass wall will affect the dose deposition in the gel. An ion chamber measurement is necessary to evaluate the dose at each position along the depth of the solid water phantom. The dose reduction caused by the borosilicate glass of the calibration vials amounts to 0.44% per millimetre glass.

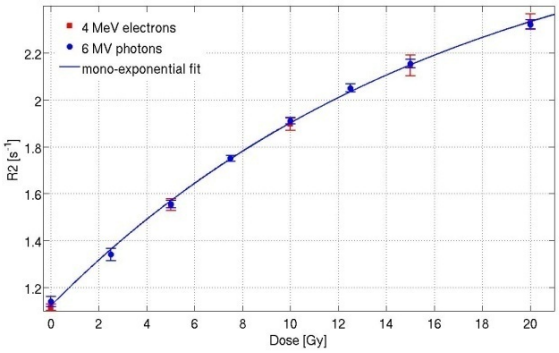

Figure 3: The dose response of calibration phantoms irradiated with 6 MV photon beam as compared to the dose response of calibration phantoms irradiated to a 4 MeV electron beam.

3.2. Electron dose measurements and simulations

In figure 4, nineteen electron trajectories are shown corresponding to the nineteen energy bins used in the simulations. A total of 1000 electron trajectories were simulated. In figure 5, a comparison between the simulated dose distribution and the gel measured dose distribution is displayed. The simulations were rescaled to the measured dose values in the gel. Because no interaction with matter is included in the simulation, actual dose maps were not calculated. Figure 5a and 5b display the simulated entrance fluence maps. Figure 5c and 5d display the gel measured entrance dose maps. A good agreement with the simulations is found.

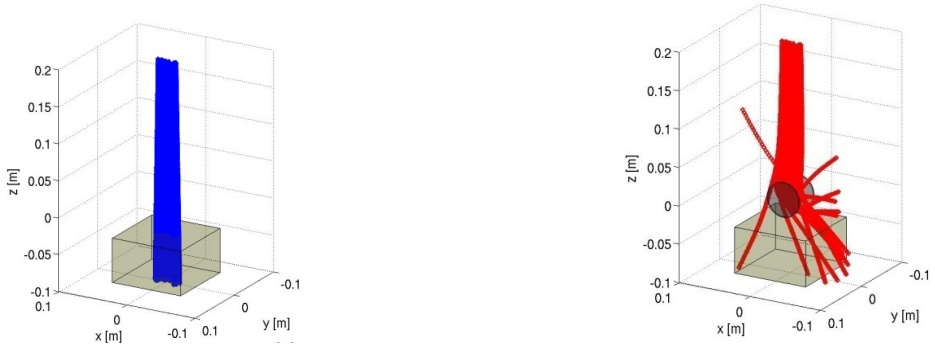

Figure 4: Nineteen electron trajectories are shown corresponding to the nineteen energy bins used in the simulations without an external magnetic field (a) and with and external magnetic field applied (b).

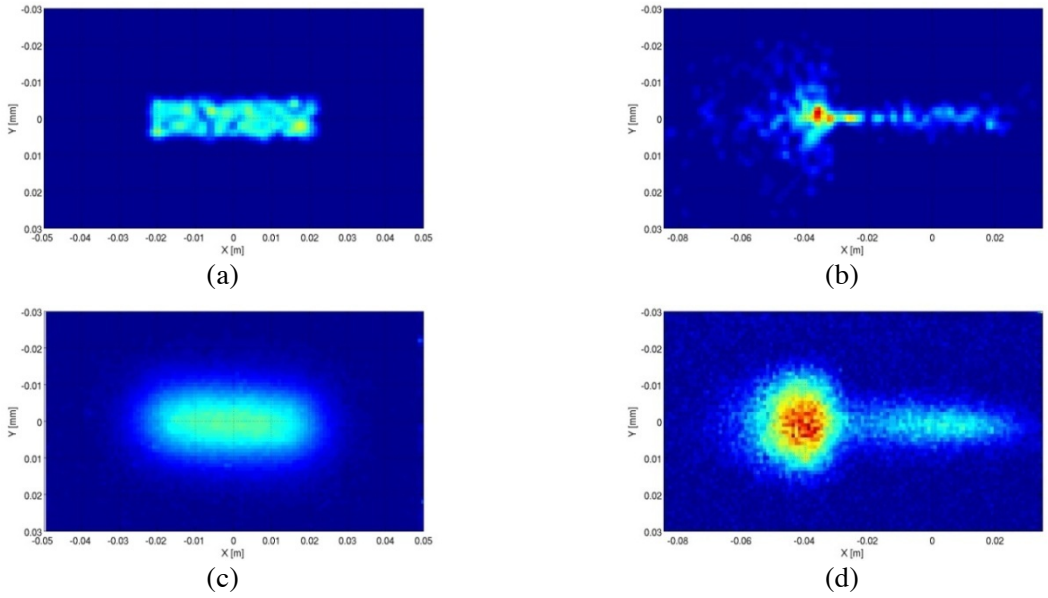

Figure 5: Results of the simulation of a 4 x 1 cm² 4 MeV electron beam without (a) and with (b) an external magnetic field applied. In c and d the polymer gel dosimetry measurements are shown.

4. Conclusions

Simulations and gel measurements are in good agreement. In future work, lung equivalent gel dosimeters will be used in a strong magnetic field to investigate the influence of the applied magnetic field on the 3D dose distribution and Monte-Carlo simulations will be applied to incorporate the particle interactions in the phantom.

5. Acknowledgements

This research is supported by the Institute for the Promotion of Innovation though Science and Technology in Flanders (IWT -Vlaanderen).

6. References

[1] Raaijmakers A J E *et al* 2007 *Phys. Med. Biol.* **52** 7045-54
[2] Aubin J *et al* 2010 *Phys. Med. Biol.* **55** 4861-9
[3] Raaymakers B W *et al* 2007 *Phys. Med. Biol.* **49** 4109-118
[4] De Deene Y *et al* 2006 *Med. Phys.* **33**, 2586-97.

[5] De Deene Y *et al* 2006 *Phys. Med. Biol.* **51** 653-73
[6] Kovar I *et al* 1983 *Phys. Med. Biol.* **28** 1441-6
[7] De Deene Y *et al* 1998 *Signal Process* **70** 85-101